ARCHIVES OF ACOUSTICS
22, 3, 351–357 (1997)

# OBSERVATION OF HYPERSONIC ACOUSTIC WAVES IN A $LiTaO_3$ CRYSTAL

T. BŁACHOWICZ and Z. KLESZCZEWSKI

Institute of Physics
Silesian Technical University
(44-100 Gliwice, ul. Krzywoustego 2)

In this paper, we would like to present theoretical considerations and results of the observation of acoustic quasi-longitudinal and quasi-transverse waves in a sample of known crystalographic orientation. The Brillouin light scattering method is suitable for investigations of the acoustic properties of materials in the hypersonic range. Results of the calculation based on ultrasonic data are not in agreement with experimental hypersonic measurements. We have observed a dispersion in the velocity of the acoustic waves.

## 1. Introduction

The Brillouin light scattering experiment has been well known for many years as a very sensitive method for studying phonons from acoustic branch in the hypersonic range, both in transparent (bulk phonons) [1, 2, 3, 4] and nontransparent media (surface phonons) [5, 6].

From the clasical point of view, the effect of scattering is connected with the Doppler shift in frequency caused by interaction between the electromagnetic and the driving acoustic waves. The elementary source of scattered light is a radiating dipole induced by the light wave. However, the most important feature are the space-time changes in the dielectric constant tensor of the investigated material. From the quantum point of view, the creation and annihilation processes of phonons by photons are responsible for a typical picture in that Brillouin lines appear.

The main problem for the experimental work is to meaure Brillouin signals in the presence of the elastically scattered light. In our case a single photon counting method was used. We would like to present results of measurements of velocity and frequency of the acoustic wave in piezoelectric $LiTaO_3$ crystal. Theoretical predictions were based on ultrasonic data.

## 2. Theoretical calculations

There are two main principles for performing the calculations. The first one is the second Newton's law describing the propagation of an acoustic wave in any direction

of the crystal. The second one is the momentum conservation law which connects the momentum wave vector of the incident light $\mathbf{k}$ with the wave vector of the scattered light $\mathbf{k}'$ and with the wave vector of the acoustic wave $\mathbf{q}$

$$\mathbf{q} = \mathbf{k}' - \mathbf{k}. \tag{2.1}$$

For the geometry of scattering presented in Fig. 1 we have

$$\begin{aligned} q_x &= k'_x - k_x\,, \qquad q_y = k'y - k_y\,, \qquad k'_x = k'\cos\alpha\,, \\ k'_y &= k'\sin\alpha, \qquad k_x = -k\sin\alpha, \qquad k_y = k\cos\alpha, \\ q_x &= k'\cos\alpha + k\sin\alpha \cong k(\sin\alpha + \cos\alpha), \\ q_y &= k'\sin\alpha - k\cos\alpha \cong k(\sin\alpha - \cos\alpha), \end{aligned} \tag{2.2}$$

where $\alpha$ is the angle between the [100] crystalographic axis and the direction of scattering. We can define the unit wave vector of the acoustic wave as

$$\boldsymbol{\chi} = \frac{\mathbf{q}}{q}; \tag{2.3}$$

from this point we can change the letter notation to the number one. Thus we have

$$\chi_1 = \chi_x = \frac{\sqrt{2}}{2}(\sin\alpha + \cos\alpha) \qquad \chi_2 = \chi_y = \frac{\sqrt{2}}{2}(\sin\alpha - \cos\alpha), \qquad \chi_3 = \chi_z = 0. \tag{2.4}$$

with the obvious condition for those vectors $\chi_1^2 + \chi_2^2 = 1$.

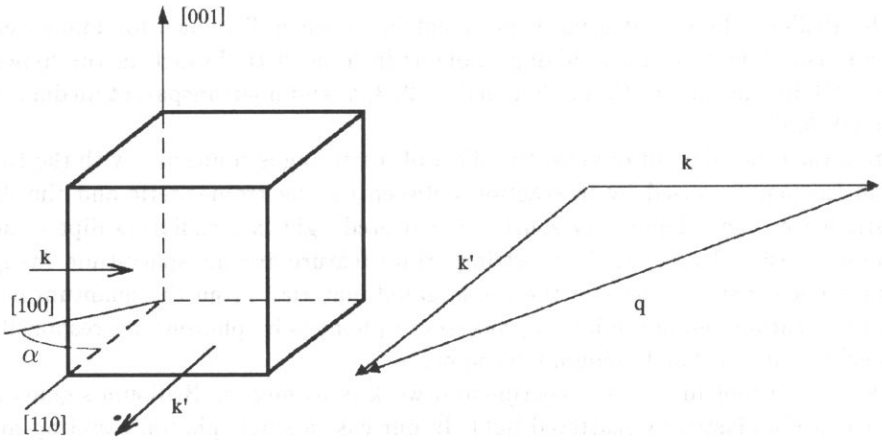


Fig. 1. Geometry of the scattering; $\alpha$ is the angle between the [100] crystalographic axis and the direction of scattering.

Detailed calculations of the expected values of frequencies, velocities and the kind of polarization of the acoustic wave can be find in [7] and in our earlier work [8]. Let us show the basic elements of the algorithm of calculations. By solving the equation of motion

$$\varrho\frac{\partial^2 u_i}{\partial t^2} = \frac{\partial}{\partial x_j}T_{ij} \tag{2.5}$$

(where $\varrho$ is the material density, $u_i$ is the vector of displacement caused by the acoustic wave and $T_{ij}$ is the stress tensor connected by the Hook's law with strains represented by the strain tensor and the stress induced electric field

$$T_{ij} = c^{ef}_{ijkl} S_{kl} - e_{nij} E_n \tag{2.6}$$

in that the piezoelectric tensor $e_{nij}$ appears) and modifying by the piezoelectric effect, the effective elastic constants are [9]

$$c^{ef}_{ijkl} = c_{ijkl} + \frac{e_{pij} e_{qkl} \chi_p \chi_q}{\varepsilon^S_{mn} \chi_m \chi_n} . \tag{2.7}$$

In the above formula the elements of the unit wave vector of the acoustic wave $\boldsymbol{\chi}$ become visible (see Eq. (2.4)). By substitution (2.7) to (2.6) and both those equations to (2.5), the following condition is obtained:

$$\det [Q_{ik} - X_i \delta_{ik}] = 0, \tag{2.8}$$

where the tensor $Q_{ik} = c^{ef}_{ijkl} \chi_j \chi_l$ is called the characteristic matrix the eigenvectors of which describe the kind of polarization, while the eigenvalues $X_i = \varrho v_i^2$ inform about the velocities of the acoustic waves. For our configuration of scattering the effective elastic constants are as follows [10]:

$$\begin{aligned}
c^{ef}_{11} &= c_{11} + \frac{e_{21} e_{21} (\sin\alpha - \cos\alpha)^2}{2\varepsilon_{11}}, & c^{ef}_{24} &= -c_{14} + \frac{e_{22} e_{24} (\sin\alpha - \cos\alpha)^2}{2\varepsilon_{11}}, \\
c^{ef}_{22} &= c_{11} + \frac{e_{22} e_{22} (\sin\alpha - \cos\alpha)^2}{2\varepsilon_{11}}, & c^{ef}_{56} &= c_{14} + \frac{e_{15} e_{16} (\sin\alpha + \cos\alpha)^2}{2\varepsilon_{11}}, \\
c^{ef}_{12} &= c_{12} + \frac{e_{21} e_{22} (\sin\alpha - \cos\alpha)^2}{2\varepsilon_{11}}, & c^{ef}_{21} &= c_{12} + \frac{e_{22} e_{21} (\sin\alpha - \cos\alpha)^2}{2\varepsilon_{11}}, \\
c^{ef}_{44} &= c_{44} + \frac{e_{24} e_{24} (\sin\alpha - \cos\alpha)^2}{2\varepsilon_{11}}, & c^{ef}_{55} &= c_{44} + \frac{e_{15} e_{15} (\sin\alpha + \cos\alpha)^2}{2\varepsilon_{11}}, \\
c^{ef}_{14} &= c_{14} + \frac{e_{21} e_{24} (\sin\alpha - \cos\alpha)^2}{2\varepsilon_{11}}, & c^{ef}_{41} &= c_{14} + \frac{e_{24} e_{21} (\sin\alpha - \cos\alpha)^2}{2\varepsilon_{11}}, \\
c^{ef}_{65} &= c_{14} + \frac{e_{16} e_{15} (\sin\alpha + \cos\alpha)^2}{2\varepsilon_{11}}, & c^{ef}_{66} &= \frac{c_{11} - c_{12}}{2} + \frac{e_{16} e_{16} (\sin\alpha + \cos\alpha)^2}{2\varepsilon_{11}}.
\end{aligned}$$

The other elastic constants are not modified by the stress induced internal electric field due to the piezoelectric effect. The elements of the characteristic matrix are as follows:

$$\begin{aligned}
Q_{11} = &\left[ c_{11} + \frac{e_{21} e_{21}}{2\varepsilon_{11}} (sin\alpha - \cos\alpha)^2 \right] \frac{1}{2} (\sin\alpha + \cos\alpha)^2 \\
&+ \left[ c_{66} + \frac{e_{16} e_{16}}{2\varepsilon_{11}} (\sin\alpha + \cos\alpha)^2 \right] \frac{1}{2} (\sin\alpha - \cos\alpha)^2, \\
Q_{22} = &\left[ c_{66} + \frac{e_{16} e_{16}}{2\varepsilon_{11}} (\sin\alpha + \cos\alpha)^2 \right] \frac{1}{2} (\sin\alpha + \cos\alpha)^2 \\
&+ \left[ c_{22} + \frac{e_{22} e_{22}}{2\varepsilon_{11}} (\sin\alpha - \cos\alpha)^2 \right] \frac{1}{2} (\sin\alpha - \cos\alpha)^2,
\end{aligned}$$

$$Q_{33} = \left[c_{55} + \frac{e_{15}e_{15}}{2\varepsilon_{11}}(\sin\alpha + \cos\alpha)^2\right]\frac{1}{2}(\sin\alpha + \cos\alpha)^2 + \left[c_{44} + \frac{e_{24}e_{24}}{2\varepsilon_{11}}(\sin\alpha - \cos\alpha)^2\right]\frac{1}{2}(\sin\alpha - \cos\alpha)^2,$$

$$Q_{23} = \left[c_{56} + \frac{e_{15}e_{16}}{2\varepsilon_{11}}(\sin\alpha + \cos\alpha)^2\right]\frac{1}{2}(\sin\alpha + \cos\alpha)^2 + \left[c_{24} + \frac{e_{22}e_{24}}{2\varepsilon_{11}}(\sin\alpha - \cos\alpha)^2\right]\frac{1}{2}(\sin\alpha - \cos\alpha)^2,$$

$$Q_{31} = \left[c_{14} + \frac{e_{21}e_{24}}{2\varepsilon_{11}}(\sin\alpha - \cos\alpha)^2 + c_{56} + \frac{e_{15}e_{16}}{2\varepsilon_{11}}(\sin\alpha + \cos\alpha)^2\right] \cdot \frac{1}{2}(\sin\alpha + \cos\alpha)(\sin\alpha - \cos\alpha),$$

$$Q_{12} = \left[c_{12} + \frac{e_{21}e_{24}}{2\varepsilon_{11}}(\sin\alpha - \cos\alpha)^2 + c_{66} + \frac{e_{16}e_{16}}{2\varepsilon_{11}}(\sin\alpha + \cos\alpha)^2\right] \cdot \frac{1}{2}(\sin\alpha + \cos\alpha)(\sin\alpha - \cos\alpha).$$

## 3. Numerical calculations

In our calculations and measurements the angle $\alpha$ is equal to 60°. The data for the calculations were taken from [11]. The results are collected in Table 1 and 2. The values of the $Q_{ik}$ characteristic matrix elements are (in $\mathrm{N/m^2}$ units)

$$Q_{ij} = \begin{bmatrix} 2.23624 \cdot 10^{11} & 3.499963 \cdot 10^{10} & -5.499941 \cdot 10^{9} \\ 3.499963 \cdot 10^{10} & 1.02376 \cdot 10^{11} & -9.52662 \cdot 10^{9} \\ -5.499941 \cdot 10^{9} & -9.52662 \cdot 10^{9} & 9.4 \cdot 10^{10} \end{bmatrix}. \tag{3.1}$$

**Table 1.** Eigenvectors of the $Q_{ik}$ matrix.

| $\gamma_1$ | $\gamma_2$ | $\gamma_3$ | polarization |
|---|---|---|---|
| −0.951566 | −0.288025 | 0.107533 | quasi-longitudinal |
| −0.253025 | 0.534991 | −0.806079 | quasi-transverse |
| −0.174642 | 0.794246 | 0.581957 | quasi-transverse |

($\boldsymbol{\gamma} = [\gamma_1, \gamma_2, \gamma_3]$ is a unit vector of the acoustic wave polarization).

**Table 2.** Velocities and frequencies of the acoustic waves.

| quasi-longitudinal | quasi-transverse $T_2$ | quasi-transverse $T_1$ | |
|---|---|---|---|
| $2.36507 \cdot 10^{11}$ | $1.20608 \cdot 10^{11}$ | $8.62634 \cdot 10^{10}$ | eigenvalues ($X = \varrho v^2$) |
| 5634.3505 | 4023.5548 | 3402.7900 | velocities [m/s] |
| 36.3423 | 25.9525 | 21.9484 | frequencies [GHz] |

## 4. Experimental investigations

The measurements were performed with the set described in detail in the articles [8, 12]. The main elements are a single mode argon laser operating at the 514.5 nm line and a pressure scanned Fabry - Perot interferometer [13]. For the detection of very weak signals the single photon counting method was applied. The measurement results were stored in the computer at one second intervals. The Brillouin spectra were performed for 75 GHz and 21.43 GHz within the full spectral range (FSR). In the first case, all kinds of acoustic waves are observed (Fig. 2), but for the second one only a quasi-longitudinal wave (Fig. 3) is seen.

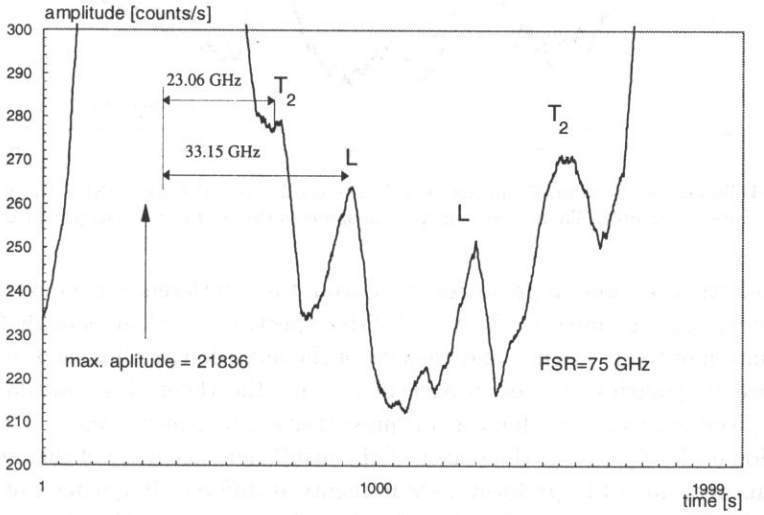


Fig. 2. Brillouin spectrum for 75 GHz within the total spectral range. The registered values of frequencies are as follows: $L = 3.15$ GHz (quasi-longitudinal wave), $T_2 = 23.06$ GHz (quasi-transverse wave). At $T_1 = 20.26$ GHz the quasi-transverse wave is not visible.

The frequency values, averaged over 8 measurements in the case of the quasi-longitudinal wave and over 4 measurements in the case of the $T_2$ quasi-transverse wave, are presented in Table 3.

**Table 3.** Measured velocities and frequencies of the acoustic waves.

| quasi-longitudinal $L$ | quasi-transverse $T_2$ | quasi-transverse $T_1$ | |
|---|---|---|---|
| $5532 \pm 73$ | $3848 \pm 153$ | | velocities [m/s] |
| $33.15 \pm 0.44$ | $23.06 \pm 0.92$ | not found | frequencies [GHz] |
| 1.3 | 2.2 | | relative uncertainty [%] |

If we compare the Brillouin spectrum for 21.43 GHz and 75 GHz FSR, we can see that the first one is a more suitable for the longitudinal wave observation and it improves the accuracy of the measurements. In the 75 GHz FSR there are stored evanescent laser

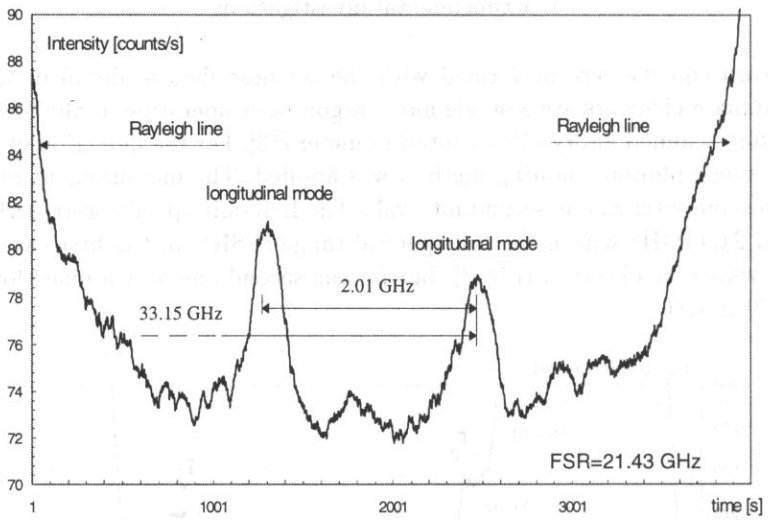


Fig. 3. Brillouin spectrum for 21.43 GHz within the total spectral range (FSR). Transverse waves are not visible. Their positions are the same as those of the Rayleigh's peaks.

modes and other accidental peaks resulting from the interference from external surfaces of the interferometer mirrors. The 21.43 GHz spectrum is clear enough for a precise determination of the frequency and velocity of the quasi-longitudinal acoustic wave. The determined frequencies are not in agreement with the theoretical calculations for the quasi-longitudinal wave and for the $T_2$ quasi-transverse acoustic wave. The lack of the observation of the $T_1$ wave is the reason of the insufficient accuracy of the measurements.

The authors intend to perform measurements at different frequencies of the acoustic waves in the same crystalographic direction in order to examine the dispersion relations.

## References

[1] GEN LI, X.K. CHEN, N.J. TAO, H.Z. CUMMINS, R.M. PICK, G. HAURET, *Brillouin scattering studies of the transverse acoustic modes of incommensurate* $K_2SeO_4$, Phys. Rev., **B 44**, 13, 6621–6629 (1991).

[2] L.E. MCNEIL, M. GRIMSDITCH, *Elastic constants of* $As_2S_3$, Phys. Rev., **B 44**, 9, 4174–4177 (1991).

[3] J.J. VANDERWAL, P. ZHAO, D. WALTON, *Brillouin scattering from the icosahedral quasi-crystal* $Al_{63.5}Cu_{24.5}Fe_{12}$, Phys. Rev., **B 46**, 1, 501–502 (1992).

[4] U. SCHÄRER, P. WACHTER, *Negative elastic constants in intermediate valent* $Sm_xLa_{1-x}S$, Solid St. Comm., **96**, 497–501 (1995).

[5] R. DANNER, R.P. HUEBENER, C.L. CHUN, M. GRIMSDITCH, I.K. SCHULLER, *Surface acoustic waves in* Ni/V *superlattices*, Phys. Rev., **B 33**, 6, 3696–3701 (1986).

[6] M. HUES, R. BHADRA, M. GRIMSDITCH, E. FULLERTON, I.K. SCHULLER, *Effect of high-energy ion irradiation on the elastic moduli of* Ag/Co *superlattices*, Phys. Rev., **B 39**, 17, 12966–12968 (1989).

[7] J.L. FABIELINSKIJ, *Molekularnoje rassiejanie sveta*, Nauka, Moskva 1965.

[8] T. BŁACHOWICZ, Z. KLESZCZEWSKI, *Experimental studies of Brillouin scattering in the* $LiTaO_3$ *crystal* [in Polish], Molecular and Quantum Acoustics, ***16***, *23–33 (1995)*.

[9] R.J. O'BRIEN, G.J. ROSACO, A. WEBER, *Brillouin scattering in Lithium Niobate*, [in:] Light scattering spectra of solids, Proceedings of the International Conference on Light Scattering Spectra of Solids, G.B. WRIGHT [Ed.], New York, September 1968, Springer Verlag, New York 1969, pp. 623–630.

[10] T. BŁACHOWICZ, Z. KLESZCZEWSKI, *Observation of the hypersonic waves in the* $LiTaO_3$ *crystal*, Molecular and Quantum Acoustics, **17**, 37–43 (1996).

[11] J. XU, R. STROUD, *Acousto-optic devices: principles, design and applications*, John Wiley and Sons Inc., New York 1992.

[12] T. BŁACHOWICZ, R. BUKOWSKI, Z. KLESZCZEWSKI, *Układ pomiarowy do badania rozpraszania Brillouina w cieczach i ciałach stałych* [in Polish], Zeszyty Naukowe Politechniki Śląskiej, **73**, 7–17 (1996).

[13] T. BŁACHOWICZ, R. BUKOWSKI, Z. KLESZCZEWSKI, *Fabry-Perot intrferometer in Brillouin scattering experiments*, Rev. Sci. Instrum., **67**, 12, 4057–4060 (1996).